

Title Page

Off-target STK10 inhibition by erlotinib enhances lymphocytic activity leading to severe skin disorders.

Naoko Yamamoto, Masashi Honma and Hiroshi Suzuki

Department of Pharmacy, The University of Tokyo Hospital, Faculty of Medicine, The University of Tokyo, Tokyo 113-8655, Japan : N.Y., M.H. and H.S.

Running Title Page

Running Title: Aggravation of skin rash via STK10 inhibition by erlotinib

Corresponding Author: Masashi Honma

Department of Pharmacy, The University of Tokyo Hospital, Faculty of Medicine,

The University of Tokyo, 7-3-1 Hongo, Bunkyo-ku, Tokyo 113-8655, Japan.

Tel: +81-3-3815-5411; Fax: +81-3-3816-6159; E-mail: mhonma-tky@umin.ac.jp.

Number of text pages 39

Number of tables 0

Number of figures 7

Number of references 51

Number of words in

Abstract 246

Introduction 750

Discussion 1719

Abbreviations

BSA, bovine serum albumin; EGFR, epidermal growth factor receptor; FBS, fetal bovine serum; GAK, Cyclin G-associated kinase; MEK1, MAPK ERK kinase-1; PMA, Phorbol 12-myristate 13-acetate; SDF-1, stromal cell-derived factor-1; SLK, Ste20-like kinase; STK10, serine/threonine kinase 10

Abstract

Skin disorders are among most common adverse events related to treatment with EGFR kinase inhibitors and, of these, erlotinib is known to cause more frequent and severe skin disease than other agents in this class. Although previous reports have shown that cutaneous manifestations are triggered by the inhibition of multiple EGFR-related homeostatic functions of the skin, this mechanism alone cannot explain the differences in frequency and severity of skin disorders caused by different kinase inhibitors. In this study, we focused on the relationship between the off-target kinase inhibition and aggravation of skin disorders. Based on calculations using reported *K_d* values and plasma drug concentrations, STK10 and SLK were selected as candidates preferentially inhibited by erlotinib over gefitinib. *In vitro* experiments confirmed that STK10 and SLK kinase activity are inhibited by erlotinib at clinical concentrations, while only STK10 is slightly inhibited by gefitinib. It was also shown that erlotinib up-regulated lymphocytic responses such as IL-2 secretion and cell migration at clinical concentrations, while gefitinib did not affect lymphocyte activity. Moreover, siRNA experiments revealed that STK10 plays a major role in up-regulation of the lymphocytic responses induced by erlotinib treatment. Finally, the role of erlotinib-induced lymphocyte activation was assessed *in vivo* using irritant hypersensitivity models. The results indicated that erlotinib aggravates cutaneous inflammatory reactions through the activation of lymphocytic responses such as IL-2 secretion and cell migration. These results demonstrated that off-target inhibition of STK10 by erlotinib enhances lymphocytic responses, which lead to the aggravation of skin inflammation.

Introduction

Erlotinib and gefitinib are low-molecular-weight tyrosine kinase inhibitors whose primary target is epidermal growth factor receptor (EGFR), and which have been used to treat patients with non-small cell lung cancer (Shepherd, et al., 2005; Kris, et al., 2003). In addition to erlotinib and gefitinib, other kinase inhibitors and monoclonal antibodies that target EGFR, including lapatinib, cetuximab and panitumumab, have also been developed and used for the treatment of various types of cancer (Geyer, et al., 2006; Bonner, et al., 2006; Van Cutsem, et al., 2007). Skin disorders, including rash, pruritus, dry skin, and acne, are among the most common adverse events observed in patients treated with these drugs (Albanell, et al., 2002; Segal and Van Cutsem, 2005). After a week of treatment with erlotinib or gefitinib, acneiform eruptions with severe pain and itching appear primarily on the face and upper trunk (Pallis, et al., 2003; Hidalgo, et al., 2001). These symptoms can worsen a patient's quality of life and can lead to the dose reduction or discontinuation of treatment with EGFR inhibitory agents (Shepherd, et al., 2005).

Many studies have examined the relationship between EGFR inhibition and the development of cutaneous side effects (Albanell, et al., 2002; Guttman-Yassky, et al., 2010). Inhibition of EGFR-mediated signaling pathways induces multiple effects in basal keratinocytes, including growth arrest, decreased migration, increased cell attachment, abnormal differentiation, apoptosis, and stimulation of inflammatory systems, all of which result in distinctive cutaneous manifestations (Kari, et al., 2003; Woodworth, et al., 2005; Mascia, et al., 2003). However, the prevalence and severity of drug-related skin disorders vary significantly among EGFR kinase inhibitors. In Japanese patients, the frequency of rash was higher in patients receiving erlotinib

(97%) (Tarceva Japanese package insert, 2010) than in those on gefitinib (63%) (Iressa Japanese package insert, 2010). Lapatinib, a dual EGFR and HER2 tyrosine kinase inhibitor used for the treatment of HER2 positive breast cancer, was reported to induce rash in 49.8% of patients in monotherapy (Toi, et al., 2009). In addition, rash severity also differs in patients taking erlotinib vs. gefitinib. In phase I/II studies of erlotinib in the Japanese population, the frequency of rash graded NCI-CTCAE G2 and G3 was 67% and 4% respectively (Tarceva Japanese package insert, 2010), while in phase II trial of gefitinib in patients composed of Japanese and non-Japanese patients, the frequency of rash graded G2 and G3 was 19% and 1% respectively (Fukuoka, et al., 2003). Moreover, the IC_{50} values for erlotinib, gefitinib and lapatinib were reported to be 2 nM, 23 nM and 11 nM, respectively (Moyer, et al., 1997; Albanell, et al., 2002; Rusnak, et al., 2001). Considering the steady state unbound plasma concentrations of each drug under clinical conditions, it is estimated that EGFR is almost completely inhibited in each case. This suggests that factors other than EGFR inhibition also contribute to the severe cutaneous side effects of erlotinib.

A few reports have described the unanticipated effects caused by the inhibition of off-target kinases. Although imatinib was designed to specifically target BCR-Abl, a gene product that cause chronic myeloid leukemia, it has been suggested that imatinib has direct effects on bone-resorbing osteoclasts and bone-forming osteoblasts through the off-target inhibition of c-fms, c-kit, carbonic anhydrase II, and platelet-derived growth factor receptor (Vandyke, et al., 2010). In another example, sunitinib, multi-target kinase inhibitor used to treat renal cell carcinoma and GIST, inhibits a number of growth factor receptors regulating both tumor cell proliferation and tumor angiogenesis (Guttman-Yassky, et al., 2010). It has been suggested that the off-target inhibition of 5'-AMP-activated protein kinase plays a central role in sunitinib

toxicity in cardiomyocytes (Kerkela, et al., 2009).

Recently, Karaman *et al.* reported comprehensive measurement of selectivity of kinase inhibitors (Karaman, et al., 2008). That analysis revealed that both gefitinib and erlotinib interact with several off-target kinases as well as with their primary target, EGFR. However, it is still unclear whether off-target inhibition by erlotinib or gefitinib plays a role in cutaneous side effects of these drugs. Here, to test that possibility, we compared off-target inhibition profiles of gefitinib and erlotinib at the steady state unbound plasma concentrations found under clinical conditions. Our findings suggest that the off-target serine/threonine kinase 10 (STK10) is inhibited much more potently by erlotinib than by gefitinib under clinical conditions. Furthermore, *in vitro* experiments showed that erlotinib enhances lymphocytic responses such as cell migration and IL-2 secretion via STK10 inhibition. Our *in vivo* observations were consistent with these *in vitro* results. These results suggest that erlotinib exacerbates skin disorders through off-target kinase inhibition.

Materials and Methods

Cell lines

293FT cells were obtained from Invitrogen and cultured in DMEM (Nacalai Tesque, Kyoto, Japan) supplemented with 10% fetal bovine serum (FBS), 2 mM L-glutamine, 100 µg/ ml penicillin and streptomycin (Invitrogen, Carlsbed, CA). Jurkat E6-1 cells were obtained from the American Type Culture Collection and cultured in RPMI 1640 (Nacalai Tesque) supplemented with 10% FBS, 100 µg/ ml penicillin and streptomycin.

Animals

Male ddY mice were purchased from Japan SLC Inc. Mice were allowed to acclimate to housing conditions for at least 7 days before handling, and were analyzed at 6 weeks of age. All animal procedures were approved by the Institutional Animal Care and Use Committee of Graduate School of Medicine, the University of Tokyo.

Calculation of occupancy rates

Mean occupancy rate (R) of the kinase by the drug under clinical conditions was calculated according to the following Michaelis-Menten type equation.

$$R = \frac{C_{p,u,ss}}{Kd + C_{p,u,ss}}$$

where $C_{p,u,ss}$ and Kd are the steady-state mean unbound plasma concentration of the drug obtained from Japanese package insert and the dissociation constant of the drug from the kinase obtained from a previous report (Karaman, et al., 2008), respectively.

Preparation of recombinant kinase

Genes encoding human serine/threonine kinase 10 (STK10) and Ste20-like kinase (SLK) were cloned using cDNA from MCF-7 cells and Jurkat E6-1 cells, respectively. Genes encoding mouse STK10 and SLK were cloned using cDNA from mouse spleens and mouse brains, respectively. Each gene was fused with a His-tag at the N-terminal and subcloned into the pcDNA3.3 vector (Invitrogen) to produce 6-His STK10/pcDNA3.3 and 6-His SLK/pcDNA3.3. 293FT cells were transfected with 6-His STK10/pcDNA3.3 or 6-His SLK/pcDNA3.3 using LipofectamineTM 2000 (Invitrogen) according to the manufacturer's protocol. Forty-eight hours after transfection, cells were lysed in a lysis buffer (phosphate buffered saline (pH8.0) containing 1% Nonidet P-40, and a protease inhibitor cocktail (Roche, Indianapolis, IN). The recombinant proteins were purified using ProfinityTM IMAC Ni-Charged Resin (BioRad, Tokyo, Japan).

In vitro kinase assay

To measure the kinase activity of STK10 and SLK, 100 ng of each recombinant protein was incubated with 1 μ g of myelin basic protein (CHEMICON, Billerica, MA) and 1 μ M ATP in kinase buffer (20 mM HEPES, 10 mM MgCl₂, 3 mM MnCl₂, and 0.1 mg/ml bovine serum albumin (BSA), pH 7.6) for 1 hr at 37°C. The remaining ATP concentration was determined using the Kinase-GloTM Plus Luminescent Kinase Assay (Promega, Madison, WI) according to the manufacturer's protocol. To determine the *IC*₅₀ values for gefitinib and erlotinib for each kinase, each compound was added to the reaction mixture at the indicated concentrations. ATP concentrations were fitted to the standard *IC*₅₀ model and *IC*₅₀ values were determined based on Powell's non-linear least square method with a uniform weighting factor using Scientist[®] software (Micomath, Saint Louis, MO).

Small interfering RNA

siRNA was designed against human STK10 and SLK using BLOCK-iT RNAi Designer (Invitrogen). Sequences were: 5'-GCC UGU CUA CCU UCG AGA A-3' for STK10 (siSTK10) and 5'-GCC AUA ACC AGA ACC UGA A-3' for SLK (siSLK). siRNA duplexes containing a di-deoxythymine overhang at the 3' terminal were synthesized (Sigma Aldrich, Saint Louis, MO). Each siRNA duplex was introduced into Jurkat E6-1 cells by electroporation using a Gene Pulser Xcell (BioRad) at a setting of 140 V, 1000 μ F, and using a 0.1 cm gap cuvette according to the manufacturer's protocol. As a negative control (siNeg), we used siPerfect[®] Negative Control (Sigma) that contains at least three miss-matches against human, mouse and rat genes.

Quantification of mRNA expression by real-time PCR

Total RNA was extracted from Jurkat E6-1 cells using RNAsolv (Omega Bio-tek, Lilburn, GA) according to the manufacturer's protocol, and the prepared RNA was reverse-transcribed with ReverTra Ace (Toyobo Engineering, Osaka, Japan). Quantitative real-time PCR was performed using SYBR GreenER qPCR SuperMix Universal (Invitrogen), a Chromo4 (Bio-Rad), and the associated software. Primers used for the quantification of gene expression were as follows: human STK10 forward primer: 5'-ATC CTG CGC CTG TCT ACC TT-3', reverse primer: 5'-GCC TTG TAA ACC TTG CCG AA-3'; human SLK forward primer: 5'-CCT CAG CCT GTT CTA ATA CCC A-3', reverse primer: 5'-GGA TTC TCA GAT TCT GGT GGC A-3'; human IL-2 forward primer: 5'-TCC TGT CTT GCA TTG CAC TAA G-3', reverse primer: 5'-CAT CCT GGT GAG TTT GGG ATT C-3'; and β -actin forward primer: 5'-CCG

GAA GGA AAA CTG ACA GC-3', reverse primer: 5'-GTG GTG GTG AAG CTG TAG CC-3'.

The relative expression level of each gene was normalized to that of β -actin.

Western blotting

Forty eight hours after siRNA introduction into Jurkat E6-1 cells, whole cell lysates were prepared with phosphate buffered saline containing 1% NP-40 (lysis buffer). Proteins (20 μ g/lane) were separated on 7.5% of SDS-polyacrylamide gels and transferred onto immobilon membranes (Millipore, Billerica, MA). After a blocking treatment with Tris buffered saline containing 3% bovine serum albumin, membranes were incubated with anti-human STK10 antibody or anti-human SLK antibody (BETHYL, Montgomery, TX) as primary antibodies. As the secondary antibody, anti-rabbit IgG antibody labeled with horseradish peroxidase (GE Healthcare, Chalfont St. Giles, Buckinghamshire, UK) was used. ECL plus (GE Healthcare) was used for detection according to the manufacturer's protocol and analyzed using a Chemidoc XRS (Bio-Rad, Hercules, CA).

Measurement of IL-2 by enzyme-linked immunosorbent assay (ELISA)

Jurkat E6-1 cells were seeded on a 96-well plate at a density of 1×10^5 cells per well for stimulation with Dynabeads[®] Human T-Activator CD3/CD28 (Veritas, Tokyo, Japan) at a ratio of 3 beads to 1 cell. Lymph node cells isolated from ddY mice were seeded on a 96-well plate at a density of 1×10^5 cells per well for stimulation with Dynabeads[®] Mouse T-Activator CD3/CD28 (Veritas) at a ratio of 1 bead to 1 cell. For co-stimulation experiments with PMA (20 ng/ml) and ionomycin (1 μ M), both Jurkat cells and lymph node cells were seeded at a density of 2×10^5 cells per well. The indicated concentrations of gefitinib, erlotinib and/or PD098059 (50 μ M)

were added to the media at 1 hr before beads stimulation. In the siRNA experiments, we added erlotinib or gefitinib to the media at unbound concentrations of 400 nM and 150 nM, respectively, which are around the maximum unbound plasma concentrations of these drugs. Cell culture supernatants were collected 48 hr after stimulation and interleukin-2 (IL-2) concentration was measured by using the Quantikine Human IL-2 immunoassay (R&D Systems, Minneapolis, MN) according to the manufacturer's protocol.

Measurement of IL-2 mRNA

Jurkat E6-1 cells were seeded on a 12-well plate at a density of 4×10^5 cells per well. Bead stimulation and treatment with gefitinib and erlotinib were performed as described above. Cell pellets were collected 5 hr after bead stimulation, and IL-2 mRNA was measured using quantitative PCR.

Cell migration assay

Jurkat E6-1 cells were serum-starved and gefitinib or erlotinib were added to the medium at the indicated concentrations 1 hr before the cell migration assay. The migration assay was performed using a transwell system with a polycarbonate membrane with a 5- μ m pore (Corning, Corning, NY). Jurkat E6-1 cells were seeded on the upper chamber of each transwell at a density of 1×10^7 cells per well, and the lower chamber was filled with medium containing 10 ng/mL stromal cell-derived factor-1 (SDF-1, PeproTech, Rocky Hill, NJ) and 0.1 mg/ml BSA. Gefitinib and erlotinib were added to the upper and lower chambers at the indicated concentrations. Cells were incubated at 37°C for 2 hr, and cells that migrated into the lower chamber were counted with a hemocytometer. For gene knockdown experiments, the cell

migration assay was performed 24 hr after the addition of siRNA. SDF-1 was added at a concentration of 30 ng/mL.

Quantification of erlotinib and gefitinib using LC-MS/MS

LC-MS/MS analyses were conducted using a Quattro Premier XE Tandem Quadrupole Mass Spectrometer coupled to an ACQUITY Ultra Performance LC System with an integral autoinjector (Waters, Milford, MA). The Premier XE was run in the ESI positive - MS/MS MRM mode at a source temperature of 120°C and a desolvation temperature of 350°C by monitoring the following mass transitions (parent to daughter ion): m/z 447.43 to 127.8 for gefitinib, m/z 394.43 to 278.2 for erlotinib, and m/z 268.23 to 116.03 for metoprolol, which was used as an internal standard. The cone voltage was set at 45 V for gefitinib, 55 V for erlotinib, and 35 V for metoprolol. Plasma samples were deproteinized with 4 volumes of acetonitrile (Nacalai Tesque) and the supernatants were separated on an ACQUITY UPLC BEH Shield RP18 1.7- μ m, 2.1 \times 100-mm column (Waters) with a flow rate of 0.4 ml/min and a binary solvent system of water-acetonitrile containing 0.1% formic acid. Data analyses were carried out using MassLynx software (ver. 4.1) and quantified using sample peak area.

Pharmacokinetic analysis

Each mouse was orally administered erlotinib (t = 0 hr: 18 mg/kg, t = 6, 12, 18 hr: 13 mg/kg) or gefitinib (t = 0 hr: 25 mg/kg, t = 6, 12, 18 hr: 18 mg/kg) dissolved in saline containing 25 % methyl- β -cyclodextrin (Wako, Osaka, Japan). This dosing schedule was designed to sustain the inhibition rate of mouse STK10 by erlotinib or gefitinib in ddY mice at a level comparable to that of human STK10 under clinical conditions. The STK10 inhibition rate at each time point

was calculated based on the IC_{50} values determined from *in vitro* kinase assays and the plasma concentration of erlotinib or gefitinib which was measured using LC-MS/MS. Plasma samples were collected from the jugular vein at the indicated times. Plasma proteins were precipitated with 4 volumes of acetonitrile, and the supernatants were evaporated at 40°C under nitrogen gas flow. The pellets were dissolved in 10% acetonitrile and used for quantification.

Irritant dermatitis model

Each mouse was orally administered erlotinib (t = 0 hr: 18 mg/kg, t = 6, 12, 18 hr: 13 mg/kg) or gefitinib (t = 0 hr: 25 mg/kg, t = 6, 12, 18 hr: 18 mg/kg) dissolved in saline containing 25 % methyl- β -cyclodextrin (Wako). To elicit irritant dermatitis, 25 μ l of 5 % croton oil dissolved in acetone/olive oil (v/v = 5/1) was applied to both sides of each ear 1 hr after the first administration of gefitinib and erlotinib. To evaluate the contribution of IL-2 to dermatitis, 500 μ g/kg anti-IL-2 mAb (clone JES6-1A12, R&D systems) was injected intravenously just before croton oil treatment. To evaluate the effect of lymphocyte suppression, 3 mg/kg FTY720 (CAYMAN, Ann Arbor, MI) was orally administered on days -2, -1, and 0. The degree of earflap swelling was measured 24 hr after irritant application. Infiltration of lymphocytes to the earflaps was also quantitated. For this experiment, treatment with erlotinib or gefitinib and irritant application were performed as described above, and mice were sacrificed 6 hr after irritant challenge. The earflaps were excised and fixed in phosphate buffered saline containing 4% paraformaldehyde. The tissues were embedded in paraffin, and then, longitudinal thin sections were prepared for staining with hematoxylin-eosin as described previously. In one-third, half and two-thirds distances from the base to the tip of earflap sections along with long axis, areas with 200 μ m width were selected and infiltrated lymphocytes were counted.

Statistical Analyses

All data are expressed as means \pm SD from at least 3 independent experiments. Statistical analysis was performed using a Student's t-test or an analysis of variance (ANOVA) followed by Bonferroni's test where applicable.

Results

Comparison of off-target kinase occupancy rates in erlotinib and gefitinib at clinical levels

To compare the off-target interaction profiles of erlotinib and gefitinib, we calculated their occupancy rates for 317 types of human kinases based on a previous report of high-throughput measurements of the K_d values of various kinase inhibitors for human kinases (Karaman, et al., 2008), taking into account the steady state mean unbound plasma concentration of these agents under clinical conditions (Nakagawa, et al., 2003; Yamamoto, et al., 2008) (Fig. 1). It was estimated that both erlotinib and gefitinib occupy EGFR almost completely (100% by erlotinib and 99% by gefitinib). Cyclin G-associated kinase (GAK) was also estimated to be highly occupied by both agents (99% by erlotinib and 84% by gefitinib). In contrast, the estimated occupancy rates for STK10 and SLK were much higher for erlotinib than for gefitinib (92% by erlotinib and 12% by gefitinib for STK10, and 89% by erlotinib and 7% by gefitinib for SLK). It has been reported that both STK10 and SLK are members of the Ste20 family of serine/threonine protein kinases, and STK10 is reported to be expressed predominantly in lymphocytes (Walter, et al., 2003) and to negatively regulate lymphocytic responses such as IL-2 expression and cell migration (Tao, et al., 2002; Belkina, et al., 2009). Given that the up-regulation of lymphocytic activity is likely to lead to the aggravation of inflammatory reactions, including skin disorders, we focused on STK10 and SLK in subsequent experiments.

Determination of IC_{50} values for STK10 and SLK by erlotinib and gefitinib

To confirm that STK10 and SLK kinase activity was actually inhibited by erlotinib under clinical conditions, we determined the IC_{50} values of erlotinib and gefitinib for human STK10,

SLK, and their mouse orthologues using an *in vitro* kinase assay system (Fig. 2). The results indicated that erlotinib inhibited STK10 and SLK more potently than gefitinib under clinical conditions. The IC_{50} values of erlotinib and gefitinib for human STK10 were 160 nM and 1,300 nM, respectively, and those for mouse STK10 were 350 nM and 1,900 nM, respectively (Figs. 2A&B). The IC_{50} values of erlotinib and gefitinib for human SLK were 830 nM and 5,200 nM, respectively, and those for mouse SLK were 480 nM and 1,600 nM, respectively (Figs. 2C&D). Based on these results, it was estimated that the inhibition rate for STK10 is approximately 60% for patients treated with erlotinib, but only 4% for patients treated with gefitinib. The inhibitory effects on SLK were estimated to be somewhat lower than those on STK10, and it was estimated that the inhibition rate was approximately 25% for patients treated with erlotinib and minimal for those treated with gefitinib.

Erlotinib up-regulates IL-2 secretion and cell migration activity in lymphocytes

As mentioned above, it has been suggested that STK10 negatively regulate lymphocytic activity (Tao, et al., 2002; Belkina, et al., 2009). Therefore, we speculated that the possibility that the preferential inhibition of STK10 or SLK, which is closely related to STK10, by erlotinib might enhance lymphocyte action. To compare the effects of erlotinib and gefitinib on lymphocytic IL-2 secretion, we measured IL-2 in the media by ELISA 48 hr after the activation of Jurkat E6-1 cells, which were derived from a human lymphocytic cell line. These cells were activated with CD3/CD28-coated beads, which mimic the role of antigen presenting cells during *in vivo* T cell activation (Fig. 3A). Addition of erlotinib to the media resulted in a dose-dependent increase in IL-2 secretion, while gefitinib had little or no effect. Unfortunately, we could not determine the EC_{50} values, since the viability of the cells tended to decrease over

the 48 hr period in which higher concentrations of erlotinib or gefitinib were added to the media. However, these results suggested that erlotinib up-regulates secretion of IL-2 from lymphocytes at clinical concentrations.

Next, we examined the effects of erlotinib and gefitinib on lymphocytic cell migration using a transwell chemotaxis assay system (Fig. 3B). Addition of both erlotinib and gefitinib to the media led to an increase in the number of cells attracted by chemokines; however, erlotinib activated cell migration more potently than gefitinib. In this assay, cells were incubated for 2 hr and EC_{50} values were determined. The EC_{50} values for lymphocytic cell migration were 470 nM for erlotinib and 1,400 nM for gefitinib. The relative E_{max} values were 1.9 for erlotinib and 1.7 for gefitinib.

STK10 inhibition plays a major role in the up-regulation of lymphocytic activation by erlotinib.

We next examined the effects of RNAi gene suppression of STK10 and SLK to further establish whether the inhibition of STK10 or SLK by erlotinib mediates the up-regulation of lymphocyte action. Knockdown efficiency was confirmed by measuring mRNA and protein levels using quantitative real time PCR and western blotting, respectively, in Jurkat E6-1 cells after siRNA was introduced by electroporation (Fig. 4A&B). Since it was previously reported that IL-2 production is negatively regulated by STK10 at the transcriptional level (Tao, et al., 2002), we examined the effects of gene suppression on IL-2 mRNA expression. IL-2 mRNA expression was increased 2-fold after stimulation with CD3/CD28-coated beads in Jurkat E6-1 cells treated with siSTK10 relative to cells treated with siNeg, but no significant difference was observed in cells treated with siSLK vs. siNeg (Fig. 4C). Moreover, the addition of erlotinib at

clinical concentrations resulted in increased IL-2 mRNA expression under SLK knockdown and control conditions; however, it did not significantly affect IL-2 mRNA under STK10 knockdown conditions (Fig. 4C). Changes in IL-2 protein in the media were consistent with these changes in mRNA (Fig. 4D). These results suggest that up-regulation of IL-2 secretion in response to erlotinib is due to transcriptional up-regulation mediated by the inhibition of STK10 by erlotinib.

We next performed a transwell migration assay using Jurkat E6-1 cells under the various siRNA conditions (Fig. 4E). STK10 knockdown increased the number of cells attracted by chemokines compared to control and SLK knockdown conditions. As was the case for IL-2 production, the addition of erlotinib to the media at clinical concentrations resulted in increased chemokine-induced cell migration, while no significant change was observed under STK10 knockdown conditions (Fig. 4E). These results suggest that the up-regulation of lymphocytic action by erlotinib is largely mediated by STK10 inhibition.

Erlotinib does not affect the MEK1 pathway or Ca²⁺ signaling pathway.

It has been reported that MAPK ERK kinase-1 (MEK1) increases the IL-2 gene transcription (Whitehurst and Geppert, 1996). To confirm whether the modulation of MEK1 is the cause of high level of IL-2 secretion in response to erlotinib, the involvement of MEK1 in increased IL-2 secretion by erlotinib was investigated using the MEK1 selective inhibitor, PD098059. In the case of Jurkat E6-1 cells stimulated with CD3/CD28 beads, PD098059 partially inhibited the secretion of IL-2. The resistant remainder is thought to be dependent on signaling pathways other than the MEK1/ERK pathway. Moreover, erlotinib stimulated IL-2 secretion significantly even in cells co-treated with PD098059 (Fig. 5A). These results suggest that the increased IL-2 secretion induced by erlotinib treatment is mediated by the signals other than MEK1 signals. In

addition, we also measured the IL-2 secretion in cells under PMA/ionomycin co-stimulation, which bypassed the T cell receptor (TCR) signaling to activate Ras and calcineurin (Franklin, et al., 1994; Chatila, et al., 1989). Upon PMA/ionomycin co-treatment, PD098059 strongly inhibited IL-2 secretion whereas erlotinib did not (Fig. 5B). This result suggests that IL-2 secretion triggered by PMA/ionomycin co-stimulation depends more strongly on MEK1 signaling than on CD3/CD28 stimulation, and also suggests that erlotinib does not affect the MEK1 pathway or Ca^{2+} signaling pathway.

Administration of erlotinib exacerbates irritant-induced skin inflammation.

Our *in vitro* experiments indicated the preferential inhibition of STK10 by erlotinib enhances the lymphocytic response leading to the aggravation of skin disorders. To confirm this, we performed an *in vivo* irritant hypersensitivity assay using male ddY mice. In these experiments, the swelling of earflaps 24 hr after topical application of croton oil was used as an indicator of irritant hypersensitivity, and erlotinib or gefitinib was orally administered 4 times over 24 hr. The dosage regimens for erlotinib and gefitinib were designed to maintain the inhibition rate for STK10 at a similar level to that of patients treated with these agents, based on previous reports of the mouse pharmacokinetic profiles (Wang, et al., 2008; Marchetti, et al., 2008) and the IC_{50} values for human and mouse STK10 measured in the present study (Fig. 2). To confirm the STK10 inhibition profiles, we measured plasma concentrations of erlotinib and gefitinib at the indicated time points and compared the estimated STK10 inhibition profiles in mice and humans (Figs. 6A&B). Earflap swelling was significantly exacerbated by erlotinib administration compared to controls, but gefitinib administration did not affect earflap swelling (Fig. 6C).

In order to confirm that mouse lymphocytes responses are actually affected by erlotinib as

seen in human cell line, Jurkat-E6-1 cells, we also determined the effect of erlotinib and gefitinib on IL-2 secretion *in vitro* using lymph node cells from ddY mice. Upon stimulation with CD3/CD28 beads, the addition of erlotinib to the media resulted in a dose-dependent increase in IL-2 secretion, while gefitinib had no effect on lymph node cells at concentration used in clinical situations (Fig. 6D). In addition, erlotinib and gefitinib had no effect on the secretion of IL-2 in lymph node cells upon PMA/ionomycin co-stimulation (Fig. 6E). These results indicate that erlotinib exhibits similar lymphocytic activation properties in both Jurkat E6-1 cells and mouse lymph node cells. However, IL-2 secretion in response to PMA/ionomycin co-stimulation or CD3/CD28 bead stimulation was higher in lymph node cells than in Jurkat-E1 cells (Fig. 3). Several possibilities can be advanced to explain this point. Jurkat-E1 is an immortalized cell line that was cultured alone, while the lymph node cells were freshly isolated from mice as a mixture of several types of cells, including lymphocytes, macrophages and dendritic cells. In general, physiological reactions of immortalized cell line often proceed weakly compared to the case of primary cultured cells. Thus, we think it is plausible that lymph node cells were more strongly activated than Jurkat cells, although Jurkat cells maintain their ability to produce IL-2 in response to stimulation. In addition, IL-2 production from T cells after stimulation might be up-regulated via crosstalk with other types of cells in the case of isolated lymph node cells.

Activation of lymphocytic responses mediates the exacerbation of skin inflammation by erlotinib treatment.

We also measured lymphocyte infiltration in earflaps by tissue section staining. Only erlotinib treatment increased lymphocyte infiltration in the inflamed area (Fig. 7A). To confirm our *in vitro* finding of the up-regulation of IL-2 secretion and lymphocyte migration in response

to erlotinib treatment, we administered anti-IL-2 antibody or FTY720, an immunosuppressant sequestering T lymphocytes within peripheral lymphoid tissues, to mice treated with the irritant. Treatment with anti-IL-2 antibody or FTY720 reduced earflap swelling in erlotinib-treated animals (Figs. 7B&C). These results indicate that the up-regulation of lymphocytic activation by erlotinib treatment contributes to the aggravation of skin inflammation.

Discussion

A limited number of reports have focused on the inhibition of off-target kinases by clinically used kinase inhibitors (Bain, et al., 2007; Karaman, et al., 2008). These reports have only addressed the magnitude of off-target K_d values or selectivity scores, which represent the ratio of off-target and primary target K_d values, and the pharmacokinetic properties of these anti-cancer agents have not been considered. However, the off-target kinase inhibition rate is directly correlated with the development of adverse effects. The off-target inhibition rate for a kinase inhibitor which shows 100-fold selectivity is estimated to be 8.3% if the plasma concentration of the agent is adjusted to achieve 90.0% inhibition of the primary target. It appears that 100-fold selectivity is safe enough in this case. However, if the inhibition rate for the primary target is adjusted to 99.5%, the off-target kinase inhibition rate is estimated to increase to 66.6%, possibly resulting in adverse effects. This estimation also demonstrates that the off-target inhibition rate shows large variability depending on the plasma concentration of the drug. For cytotoxic anti-cancer agents, clinical doses are typically determined based on the maximum tolerated dose estimation (Sleijfer and Wiemer, 2008). However, this is not always the case for tyrosine kinase inhibitors, and the primary target inhibition rates achieved at clinical doses vary among kinase inhibitors. For imatinib, the inhibition rate for Bcr-Abl, the primary target of this agent, is estimated to be 90% based on the reported IC_{50} value and the steady-state unbound plasma concentration (Deininger, et al., 2005). For erlotinib and gefitinib, which are the focus of this study, the EGFR inhibition rates are estimated to be 100% and 99%, respectively (Fig. 1). Therefore, it is necessary to convert K_d or IC_{50} values for off-target kinases into inhibition rates at clinical concentrations taking into consideration the pharmacokinetic properties of tyrosine

kinase inhibitors.

In the present study, we focused on the relationship between off-target kinase inhibition and the aggravation of skin disorders, focusing on two kinase inhibitors that primarily target EGFR, erlotinib and gefitinib. Based on estimations of human kinase occupancy by erlotinib and gefitinib, we determined that erlotinib interacts strongly with GAK, STK10, and SLK, as well as EGFR (Fig. 1). A number of studies have described the involvement of EGFR inhibition in the pathophysiological mechanisms of cutaneous toxicity observed in patients treated with EGFR kinase inhibitors (Lacouture, 2006). The primary event is damage to the sebaceous glands and follicular epithelia, which leads to altered epidermal growth and differentiation. These cellular and structural changes subsequently trigger the release of chemokines, leading to the infiltration of mononuclear leucocytes including T lymphocytes, inflammatory dendritic cells and macrophages to the lesion area (Guttman-Yassky, et al., 2010). Histological findings show that the earliest change is the infiltration of T lymphocytes immunoreactive for CD45RO, a marker of T lymphocyte activation, which is followed by abundant neutrophil infiltration (Busam, et al., 2001). T cells are believed to facilitate inflammation through a release of effector molecules (Deane and Hickey, 2009). A series of reactions, sometimes along with the bacterial infection, finally result in cutaneous injury (Guttman-Yassky, et al., 2010). However, these proposed mechanisms do not fully explain the difference in the severity of skin disorders induced by erlotinib and gefitinib.

It seems unlikely that the inhibition of GAK is involved in the aggravation of skin disorder since gefitinib also interacts strongly with GAK (Fig. 1). In addition, the frequency of skin rash in patients taking lapatinib, a kinase inhibitor primarily targeting EGFR and Her2, is comparable to that in patients taking gefitinib, despite the fact that lapatinib does not interact with GAK (Toi,

et al., 2009; Karaman, et al., 2008). In contrast, erlotinib shows a greater interaction with STK10 and SLK than gefitinib (Fig. 1). STK10 and SLK are serine/threonine protein kinases that are closely mapped in the phylogenetic tree of the Ste20 family, and STK10 is predominantly expressed in lymphocytes, while SLK is ubiquitously expressed (Walter, et al., 2003; Yamada, et al., 2000). It has been reported that STK10 negatively regulates IL-2 expression in lymphocytes at the transcriptional level and also negatively regulates cell motility through the phosphorylation of ezrin-radixin-moesin proteins (Tao, et al., 2002; Belkina, et al., 2009). Although there are reports that SLK is required for breast cancer cell motility, disassembly of actin stress fibers and radial microtubule organization, little is known about the function of SLK in lymphocytes (Roovers, et al., 2009; Burakov, et al., 2008). Considering these points, we selected STK10 and SLK as candidates for off-target inhibition leading to inflammatory responses associated with the development of skin disorders using *in vitro* and *in vivo* experimental systems.

An *in vitro* kinase assay showed that the inhibition rates for STK10 and SLK by erlotinib in the steady state are 59% and 21%, respectively, while gefitinib showed only a slight inhibition of STK10 at clinical concentrations (Fig. 2). The IC_{50} values, which we determined from our *in vitro* experiments, were somewhat higher than the reported K_d values (Moyer, et al., 1997; Albanell, et al., 2002). Differences in experimental conditions might explain this difference. We determined the IC_{50} values using enzyme kinetics data obtained in the presence of 1 μ M ATP, and the reported K_d values were determined using a high-throughput competitive binding assay (Karaman, et al., 2008). However, we confirmed that erlotinib significantly inhibits STK10 at clinical concentrations. Our cell-based assays showed that erlotinib enhances lymphocytic responses such as IL-2 secretion and cell migration (Fig. 3). The EC_{50} values of erlotinib and

gefitinib for the enhancement of cell migration were comparable to the IC_{50} values for STK10 inhibition (Fig. 3). In addition, RNAi gene suppression experiments indicated that the up-regulation of lymphocytic activity by erlotinib or gefitinib is primarily mediated by STK10 inhibition (Fig. 4). We obtained similar results by using kinase dead forms of STK10 and SLK in place of siRNA (data not shown). Considering these *in vitro* results, it can be hypothesized that the preferential inhibition of STK10 by erlotinib leads to enhanced lymphocyte migration to the lesion area and increased local IL-2 secretion.

T cell activation is induced by a series of intracellular signaling cascade initiated by signals from the TCR / CD3 complex and other co-stimulatory molecules including CD28 (Clevers, et al., 1988). CD28 provides an essential co-stimulatory signal which approximates T cell and antigen presenting cells and augments the production of IL-2 (Lenschow, et al., 1996). In our present study, we employed CD3/CD28 beads stimulation, which mimics natural TCR signaling. TCR signaling is further amplified by ZAP70, which leads to the activation of multiple pathways, including ERK, JNK, NF- κ B, p38 and NFAT, which ultimately induce IL-2 gene expression (Chu, et al., 1998). Meanwhile, co-stimulation with PMA / ionomycin bypasses the TCR signaling and activate the signaling downstream of PLC γ , a downstream effector of ZAP-70 (Franklin, et al., 1994; Chatila, et al., 1989). Since erlotinib could up-regulate the IL-2 secretion under the CD3/CD28 stimulation not upon PMA/ionomycin stimulation (Figs 5A&B), up-regulation of IL-2 secretion by erlotinib via STK10 inhibition could be dependent on the signals other than the downstream signals of PLC γ . These results are consistent with previous reports that STK10 down-regulates the IL-2 secretion upon Raji/SEE stimulation but not upon PMA/ionomycin co-treatment. The authors of this report considered that STK10 might act on early events in T cell activation (Tao, et al., 2002).

Our observations in a mouse contact hypersensitivity model were consistent with the *in vitro* observations (Fig. 6, Fig. 7). Infiltration of lymphocytes was up-regulated in the earflaps of erlotinib-treated mice compared with gefitinib- or control-treated animals (Fig. 7). Treatment with anti-IL-2 antibody or FTY720 also resulted in a reduction in earflap swelling induced by erlotinib treatment (Fig. 7). These observations are also consistent with the proposed mechanism of skin rash development in patients treated with erlotinib, in which inflammatory reactions are dominated by mononuclear leucocytes, including lymphocytes and neutrophils (Guttman-Yassky, et al., 2010).

It has been reported that there is significant inter-individual variation in plasma concentrations of erlotinib and gefitinib (Thomas, et al., 2009; Li, et al., 2006). Preclinical studies have demonstrated that CYP3A4 is primarily involved in the metabolism of erlotinib and gefitinib and, therefore, pharmacokinetic interactions may take place with drugs that inhibit or induce CYP3A4 (McKillop, et al., 2005; Li, et al., 2007). Itraconazole is a potent inhibitor of CYP3A4 and the plasma *AUC* of gefitinib was reported to increase by 78% with the co-administration of itraconazole (Swaisland, et al., 2005). Co-administration of ketoconazole, another strong inhibitor of CYP3A4, was reported to cause a two-fold increase in plasma *AUC* and the maximum plasma concentration of erlotinib (Rakhit, et al., 2008). Based on the *IC*₅₀ values obtained from our *in vitro* kinase assay and the mean unbound plasma concentrations of erlotinib and gefitinib at the steady state, it is estimated that the mean rate of STK10 inhibition was approximately 59% for erlotinib but only 4% for gefitinib (Fig. 2). If inter-individual variations in CYP3A4 activity and/or drug-drug interactions were to result in a two-fold higher unbound plasma concentration of erlotinib or gefitinib compared to the mean values, the inhibition rate for STK10 would increase to 74% for erlotinib, but would remain at 8% for gefitinib. In contrast,

the inhibition rate for EGFR, which is almost 100% for both erlotinib and gefitinib, would not be affected by these conditions. These estimations indicate that inter-individual differences in the severity of skin rash among patients treated with erlotinib may be due to inter-individual variability in the STK10 inhibition rate. This hypothesis is also supported by a previous report showing that variability in skin rash susceptibility was associated with trough erlotinib plasma concentrations (Rudin, et al., 2008).

In conclusion, we propose a mechanism in which erlotinib exacerbates skin disorders through the enhancement of lymphocytic responses such as lymphocyte migration and increased IL-2 secretion via STK10 inhibition. Since it has been demonstrated that off-target inhibition by kinase inhibitors can result in the development of adverse effects under clinical conditions, it would be beneficial to determine the comprehensive inhibitory profiles of kinase inhibitors at the preclinical stage. In cases where the inhibition rate for off-target kinases is predicted to be variable within the clinical concentration range for reasons such as inter-individual variability in pharmacokinetics and drug-drug interactions, clinical dose determination studies should be performed carefully and strategically to maximize therapeutic effects and minimize side effects.

Authorship Contributions

Participated in research design: Honma, Yamamoto and Suzuki

Conducted experiments: Yamamoto and Honma

Performed data analysis: Honma and Yamamoto

Wrote or contributed to the writing of the manuscript: Yamamoto, Honma, and Suzuki

References

- Albanell J, Rojo F, Averbuch S, Feyereislova A, Mascaro JM, Herbst R, LoRusso P, Rischin D, Sauleda S, Gee J, Nicholson RI and Baselga J (2002) Pharmacodynamic studies of the epidermal growth factor receptor inhibitor ZD1839 in skin from cancer patients: histopathologic and molecular consequences of receptor inhibition. *J Clin Oncol* **20**:110-124.
- Bain J, Plater L, Elliott M, Shpiro N, Hastie CJ, McLauchlan H, Klevernic I, Arthur JS, Alessi DR and Cohen P (2007) The selectivity of protein kinase inhibitors: a further update. *Biochem J* **408**:297-315.
- Belkina NV, Liu Y, Hao JJ, Karasuyama H and Shaw S (2009) LOK is a major ERM kinase in resting lymphocytes and regulates cytoskeletal rearrangement through ERM phosphorylation. *Proc Natl Acad Sci U S A* **106**:4707-4712.
- Bonner JA, Harari PM, Giralt J, Azarnia N, Shin DM, Cohen RB, Jones CU, Sur R, Raben D, Jassem J, Ove R, Kies MS, Baselga J, Yousoufian H, Amellal N, Rowinsky EK and Ang KK (2006) Radiotherapy plus cetuximab for squamous-cell carcinoma of the head and neck. *N Engl J Med* **354**:567-578.
- Burakov AV, Zhapparova ON, Kovalenko OV, Zinovkina LA, Potekhina ES, Shanina NA, Weiss DG, Kuznetsov SA and Nadezhdina ES (2008) Ste20-related protein kinase LOSK (SLK) controls microtubule radial array in interphase. *Mol Biol Cell* **19**:1952-1961.
- Busam KJ, Capodiec P, Motzer R, Kiehn T, Phelan D and Halpern AC (2001) Cutaneous side-effects in cancer patients treated with the antiepidermal growth factor receptor antibody C225. *Br J Dermatol* **144**:1169-1176.

- Chatila T, Silverman L, Miller R and Geha R (1989) Mechanisms of T cell activation by the calcium ionophore ionomycin. *J Immunol* **143**:1283-1289. Chu DH, Morita CT and Weiss A (1998) The Syk family of protein tyrosine kinases in T-cell activation and development. *Immunol Rev* **165**:167-180.
- Clevers H, Alarcon B, Wileman T and Terhorst C (1988) The T cell receptor/CD3 complex: a dynamic protein ensemble. *Annu Rev Immunol* **6**:629-662.
- Deane JA and Hickey MJ (2009) Molecular mechanisms of leukocyte trafficking in T-cell-mediated skin inflammation: insights from intravital imaging. *Expert Rev Mol Med* **11**:e25.
- Deininger M, Buchdunger E and Druker BJ (2005) The development of imatinib as a therapeutic agent for chronic myeloid leukemia. *Blood* **105**:2640-2653.
- Franklin RA, Tordai A, Patel H, Gardner AM, Johnson GL and Gelfand EW (1994) Ligation of the T cell receptor complex results in activation of the Ras/Raf-1/MEK/MAPK cascade in human T lymphocytes. *J Clin Invest* **93**:2134-2140.
- Fukuoka M, Yano S, Giaccone G, Tamura T, Nakagawa K, Douillard JY, Nishiwaki Y, Vansteenkiste J, Kudoh S, Rischin D, Eek R, Horai T, Noda K, Takata I, Smit E, Averbuch S, Macleod A, Feyereislova A, Dong RP and Baselga J (2003) Multi-institutional randomized phase II trial of gefitinib for previously treated patients with advanced non-small-cell lung cancer (The IDEAL 1 Trial) [corrected. *J Clin Oncol* **21**:2237-2246.
- Geyer CE, Forster J, Lindquist D, Chan S, Romieu CG, Pienkowski T, Jagiello-Gruszfeld A, Crown J, Chan A, Kaufman B, Skarlos D, Campone M, Davidson N, Berger M, Oliva C,

- Rubin SD, Stein S and Cameron D (2006) Lapatinib plus capecitabine for HER2-positive advanced breast cancer. *N Engl J Med* **355**:2733-2743.
- Guttman-Yassky E, Mita A, De Jonge M, Matthews L, McCarthy S, Iwata KK, Verweij J, Rowinsky EK and Krueger JG (2010) Characterisation of the cutaneous pathology in non-small cell lung cancer (NSCLC) patients treated with the EGFR tyrosine kinase inhibitor erlotinib. *Eur J Cancer* **46**:2010-2019.
- Hidalgo M, Siu LL, Nemunaitis J, Rizzo J, Hammond LA, Takimoto C, Eckhardt SG, Tolcher A, Britten CD, Denis L, Ferrante K, Von Hoff DD, Silberman S and Rowinsky EK (2001) Phase I and pharmacologic study of OSI-774, an epidermal growth factor receptor tyrosine kinase inhibitor, in patients with advanced solid malignancies. *J Clin Oncol* **19**:3267-3279.
- Iressa [Japanese package insert]. Osaka, Japan: AstraZeneca K.K.; 2010
- Karaman MW, Herrgard S, Treiber DK, Gallant P, Atteridge CE, Campbell BT, Chan KW, Ciceri P, Davis MI, Edeen PT, Faraoni R, Floyd M, Hunt JP, Lockhart DJ, Milanov ZV, Morrison MJ, Pallares G, Patel HK, Pritchard S, Wodicka LM and Zarrinkar PP (2008) A quantitative analysis of kinase inhibitor selectivity. *Nat Biotechnol* **26**:127-132.
- Kari C, Chan TO, Rocha de Quadros M and Rodeck U (2003) Targeting the epidermal growth factor receptor in cancer: apoptosis takes center stage. *Cancer Res* **63**:1-5.
- Kerkela R, Woulfe KC, Durand JB, Vagnozzi R, Kramer D, Chu TF, Beahm C, Chen MH and Force T (2009) Sunitinib-induced cardiotoxicity is mediated by off-target inhibition of AMP-activated protein kinase. *Clin Transl Sci* **2**:15-25.
- Kris MG, Natale RB, Herbst RS, Lynch TJ, Jr, Prager D, Belani CP, Schiller JH, Kelly K, Spiridonidis H, Sandler A, Albain KS, Cella D, Wolf MK, Averbuch SD, Ochs JJ and

- Kay AC (2003) Efficacy of gefitinib, an inhibitor of the epidermal growth factor receptor tyrosine kinase, in symptomatic patients with non-small cell lung cancer: a randomized trial. *JAMA* **290**:2149-2158.
- Lacouture ME (2006) Mechanisms of cutaneous toxicities to EGFR inhibitors. *Nat Rev Cancer* **6**:803-812.
- Lenschow DJ, Walunas TL and Bluestone JA (1996) CD28/B7 system of T cell costimulation. *Annu Rev Immunol* **14**:233-258.
- Li J, Karlsson MO, Brahmer J, Spitz A, Zhao M, Hidalgo M and Baker SD (2006) CYP3A phenotyping approach to predict systemic exposure to EGFR tyrosine kinase inhibitors. *J Natl Cancer Inst* **98**:1714-1723.
- Li J, Zhao M, He P, Hidalgo M and Baker SD (2007) Differential metabolism of gefitinib and erlotinib by human cytochrome P450 enzymes. *Clin Cancer Res* **13**:3731-3737.
- Marchetti S, de Vries NA, Buckle T, Bolijn MJ, van Eijndhoven MA, Beijnen JH, Mazzanti R, van Tellingen O and Schellens JH (2008) Effect of the ATP-binding cassette drug transporters ABCB1, ABCG2, and ABCC2 on erlotinib hydrochloride (Tarceva) disposition in in vitro and in vivo pharmacokinetic studies employing Bcrp1-/-/Mdr1a/1b-/- (triple-knockout) and wild-type mice. *Mol Cancer Ther* **7**:2280-2287.
- Mascia F, Mariani V, Girolomoni G and Pastore S (2003) Blockade of the EGF receptor induces a deranged chemokine expression in keratinocytes leading to enhanced skin inflammation. *Am J Pathol* **163**:303-312.
- McKillop D, McCormick AD, Millar A, Miles GS, Phillips PJ and Hutchison M (2005) Cytochrome P450-dependent metabolism of gefitinib. *Xenobiotica* **35**:39-50.

- Moyer JD, Barbacci EG, Iwata KK, Arnold L, Boman B, Cunningham A, DiOrio C, Doty J, Morin MJ, Moyer MP, Neveu M, Pollack VA, Pustilnik LR, Reynolds MM, Sloan D, Theleman A and Miller P (1997) Induction of apoptosis and cell cycle arrest by CP-358,774, an inhibitor of epidermal growth factor receptor tyrosine kinase. *Cancer Res* **57**:4838-4848.
- Nakagawa K, Tamura T, Negoro S, Kudoh S, Yamamoto N, Yamamoto N, Takeda K, Swaisland H, Nakatani I, Hirose M, Dong RP and Fukuoka M (2003) Phase I pharmacokinetic trial of the selective oral epidermal growth factor receptor tyrosine kinase inhibitor gefitinib ('Iressa', ZD1839) in Japanese patients with solid malignant tumors. *Ann Oncol* **14**:922-930.
- Pallis AG, Mavroudis D, Androulakis N, Souglakos J, Kouroussis C, Bozionelou V, Vlachonikolis IG and Georgoulas V (2003) ZD1839, a novel, oral epidermal growth factor receptor-tyrosine kinase inhibitor, as salvage treatment in patients with advanced non-small cell lung cancer. Experience from a single center participating in a compassionate use program. *Lung Cancer* **40**:301-307.
- Rakhit A, Pantze MP, Fettner S, Jones HM, Charoin JE, Riek M, Lum BL and Hamilton M (2008) The effects of CYP3A4 inhibition on erlotinib pharmacokinetics: computer-based simulation (SimCYP) predicts in vivo metabolic inhibition. *Eur J Clin Pharmacol* **64**:31-41.
- Roovers K, Wagner S, Storbeck CJ, O'Reilly P, Lo V, Northey JJ, Chmielecki J, Muller WJ, Siegel PM and Sabourin LA (2009) The Ste20-like kinase SLK is required for ErbB2-driven breast cancer cell motility. *Oncogene* **28**:2839-2848.

- Rudin CM, Liu W, Desai A, Karrison T, Jiang X, Janisch L, Das S, Ramirez J, Poonkuzhali B, Schuetz E, Fackenthal DL, Chen P, Armstrong DK, Brahmer JR, Fleming GF, Vokes EE, Carducci MA and Ratain MJ (2008) Pharmacogenomic and pharmacokinetic determinants of erlotinib toxicity. *J Clin Oncol* **26**:1119-1127.
- Rusnak DW, Lackey K, Affleck K, Wood ER, Alligood KJ, Rhodes N, Keith BR, Murray DM, Knight WB, Mullin RJ and Gilmer TM (2001) The effects of the novel, reversible epidermal growth factor receptor/ErbB-2 tyrosine kinase inhibitor, GW2016, on the growth of human normal and tumor-derived cell lines in vitro and in vivo. *Mol Cancer Ther* **1**:85-94.
- Segaert S and Van Cutsem E (2005) Clinical signs, pathophysiology and management of skin toxicity during therapy with epidermal growth factor receptor inhibitors. *Ann Oncol* **16**:1425-1433.
- Shepherd FA, Rodrigues Pereira J, Ciuleanu T, Tan EH, Hirsh V, Thongprasert S, Campos D, Maoleekoonpiroj S, Smylie M, Martins R, van Kooten M, Dediu M, Findlay B, Tu D, Johnston D, Bezjak A, Clark G, Santabarbara P, Seymour L and National Cancer Institute of Canada Clinical Trials Group (2005) Erlotinib in previously treated non-small-cell lung cancer. *N Engl J Med* **353**:123-132.
- Sleijfer S and Wiemer E (2008) Dose selection in phase I studies: why we should always go for the top. *J Clin Oncol* **26**:1576-1578.
- Swaisland HC, Ranson M, Smith RP, Leadbetter J, Laight A, McKillop D and Wild MJ (2005) Pharmacokinetic drug interactions of gefitinib with rifampicin, itraconazole and metoprolol. *Clin Pharmacokinet* **44**:1067-1081.

- Tao L, Wadsworth S, Mercer J, Mueller C, Lynn K, Siekierka J and August A (2002) Opposing roles of serine/threonine kinases MEKK1 and LOK in regulating the CD28 responsive element in T-cells. *Biochem J* **363**:175-182.
- Tarceva [Japanese package insert]. Tokyo, Japan: Chugai Pharmaceutical Corp.; 2010
- Thomas F, Rochaix P, White-Koning M, Hennebelle I, Sarini J, Benlyazid A, Malard L, Lefebvre JL, Chatelut E and Delord JP (2009) Population pharmacokinetics of erlotinib and its pharmacokinetic/pharmacodynamic relationships in head and neck squamous cell carcinoma. *Eur J Cancer* **45**:2316-2323.
- Toi M, Iwata H, Fujiwara Y, Ito Y, Nakamura S, Tokuda Y, Taguchi T, Rai Y, Aogi K, Arai T, Watanabe J, Wakamatsu T, Katsura K, Ellis CE, Gagnon RC, Allen KE, Sasaki Y and Takashima S (2009) Lapatinib monotherapy in patients with relapsed, advanced, or metastatic breast cancer: efficacy, safety, and biomarker results from Japanese patients phase II studies. *Br J Cancer* **101**:1676-1682.
- Van Cutsem E, Peeters M, Siena S, Humblet Y, Hendlisz A, Neyns B, Canon JL, Van Laethem JL, Maurel J, Richardson G, Wolf M and Amado RG (2007) Open-label phase III trial of panitumumab plus best supportive care compared with best supportive care alone in patients with chemotherapy-refractory metastatic colorectal cancer. *J Clin Oncol* **25**:1658-1664.
- Vandyke K, Fitter S, Dewar AL, Hughes TP and Zannettino AC (2010) Dysregulation of bone remodeling by imatinib mesylate. *Blood* **115**:766-774.
- Walter SA, Cutler RE, Jr, Martinez R, Gishizky M and Hill RJ (2003) Stk10, a new member of the polo-like kinase kinase family highly expressed in hematopoietic tissue. *J Biol Chem* **278**:18221-18228.

- Wang S, Guo P, Wang X, Zhou Q and Gallo JM (2008) Preclinical pharmacokinetic/pharmacodynamic models of gefitinib and the design of equivalent dosing regimens in EGFR wild-type and mutant tumor models. *Mol Cancer Ther* **7**:407-417.
- Whitehurst CE and Geppert TD (1996) MEK1 and the extracellular signal-regulated kinases are required for the stimulation of IL-2 gene transcription in T cells. *J Immunol* **156**:1020-1029.
- Woodworth CD, Michael E, Marker D, Allen S, Smith L and Nees M (2005) Inhibition of the epidermal growth factor receptor increases expression of genes that stimulate inflammation, apoptosis, and cell attachment. *Mol Cancer Ther* **4**:650-658.
- Yamada E, Tsujikawa K, Itoh S, Kameda Y, Kohama Y and Yamamoto H (2000) Molecular cloning and characterization of a novel human STE20-like kinase, hSLK. *Biochim Biophys Acta* **1495**:250-262.
- Yamamoto N, Horiike A, Fujisaka Y, Murakami H, Shimoyama T, Yamada Y and Tamura T (2008) Phase I dose-finding and pharmacokinetic study of the oral epidermal growth factor receptor tyrosine kinase inhibitor Ro50-8231 (erlotinib) in Japanese patients with solid tumors. *Cancer Chemother Pharmacol* **61**:489-496.

Footnotes

This work was supported in part by Grant-in-Aid for Scientific Research [Grant 21390041] and Grant-in-Aid for Scientific Research on Innovative Areas HD-Physiology [Grant 22136015] both from the Ministry of Education, Science and Culture of Japan.

Figure Legends

Figure 1. Comparison of off-target kinase occupancy rates for erlotinib and gefitinib.

Occupancy rates were calculated based on the reported K_d values of erlotinib and gefitinib for human kinases and the steady-state mean unbound plasma concentration of these agents under clinical conditions.

Figure 2. Determination of IC_{50} values for erlotinib and gefitinib for STK10 or SLK. *In*

vitro kinase assays for hSTK10 (A), hSLK (B), mSTK10 (C), and mSLK (D). Each datum represents the mean \pm SD ($n = 6$). IC_{50} values for erlotinib were 160 nM for hSTK10, 830 nM for hSLK, 350 nM for mSTK10, and 480 nM for mSLK. IC_{50} values for gefitinib were 1,300 nM for hSTK10, 5,200 nM for hSLK, 1,900 nM for mSTK10, and 1,600 nM for mSLK.

Figure 3. Erlotinib up-regulates IL-2 secretion and cell migration in lymphocytic cells.

A, Effects of erlotinib and gefitinib on IL-2 secretion in Jurkat E6-1 cells stimulated with Dynabeads Human T-Activator CD3/CD28. Each datum represents the mean \pm SD ($n = 4$). B, Effects of erlotinib and gefitinib on cell migration in Jurkat E6-1 cells induced by SDF-1. Values are presented relative to controls. Each datum represents the mean \pm SD ($n = 4$). EC_{50} values for cell migration were 470 nM for erlotinib and 1,400 nM for gefitinib. *, $P < 0.05$. **, $P < 0.01$.

Figure 4. STK10 inhibition plays a major role in the up-regulation of lymphocytic activity

by erlotinib. A, Changes of STK10 (left) and SLK (right) mRNA levels by RNAi gene suppression. Each datum represents the mean \pm SD ($n = 3$). B, Changes of STK10 (left) and

SLK (right) protein levels by RNAi gene suppression. **C**, Effects of RNAi gene suppression of STK10 or SLK on IL-2 secretion from Jurkat E6-1 cells stimulated with beads under erlotinib or gefitinib treatment conditions. Each datum represents the mean \pm SD ($n = 3$). **D**, Effects of RNAi gene suppression of STK10 or SLK on IL-2 mRNA expression in Jurkat E6-1 cells stimulated with beads under erlotinib or gefitinib treatment conditions. Each datum represents the mean \pm SD ($n = 3$). **E**, Effects of RNAi gene suppression of STK10 or SLK on the migration of Jurkat E6-1 cells induced by SDF-1 under erlotinib or gefitinib treatment conditions. Each datum represents the mean \pm SD ($n = 3$). **, $P < 0.01$.

Figure 5. Erlotinib does not affect the MEK1 pathway or Ca²⁺ signaling pathway. **A**, Effects of the MEK1 inhibitor, PD098059, on IL-2 secretion in Jurkat E6-1 cells stimulated with CD3/CD28 beads. Each datum represents the mean \pm SD ($n = 3$). **B**, Effects of the PD098059 on IL-2 secretion in Jurkat E6-1 cells stimulated with PMA/ionomycin. Each datum represents the mean \pm SD ($n = 3$).

Figure 6. Erlotinib exacerbates the skin inflammatory response to croton oil. Inhibition ratios of STK10 in ddY mice orally administered erlotinib (**A**) or gefitinib (**B**). Each datum represents the mean \pm SD ($n = 5$). The solid line represents the fitted inhibition rate profile of mSTK10 by erlotinib in the mouse model, and the dashed line represents the predicted inhibition rate profile of hSTK10 by erlotinib under human clinical conditions. **C**, Effects of erlotinib or gefitinib administration on changes in earflap swelling. Each datum represents the mean \pm SD ($n = 5$). *, $P < 0.05$. **, $P < 0.01$. **D**, Effects of erlotinib and gefitinib on IL-2 secretion in mouse lymph node cells stimulated with Dynabeads Mouse T-Activator CD3/CD28. Each

datum represents the mean \pm SD (n = 4). **E**, Effects of erlotinib and gefitinib on IL-2 secretion in mouse lymph node cells stimulated with PMA/iomomycin. Each datum represents the mean \pm SD (n = 4).

Figure 7. IL-2 secretion and lymphocyte infiltration contribute to the aggravation of the inflammatory response by erlotinib. **A**, Effects of erlotinib or gefitinib administration on earflap lymphocyte infiltration. Each datum represents the mean \pm SD (n = 3). **B**, Effects of anti-IL-2 Ab on earflap swelling aggravated by erlotinib treatment. Each datum represents the mean \pm SD (n = 6). **C**, Effects of FTY720 on the earflap swelling aggravated by erlotinib treatment. Each datum represents the mean \pm SD (n = 8). *, $P < 0.05$.

Fig.1

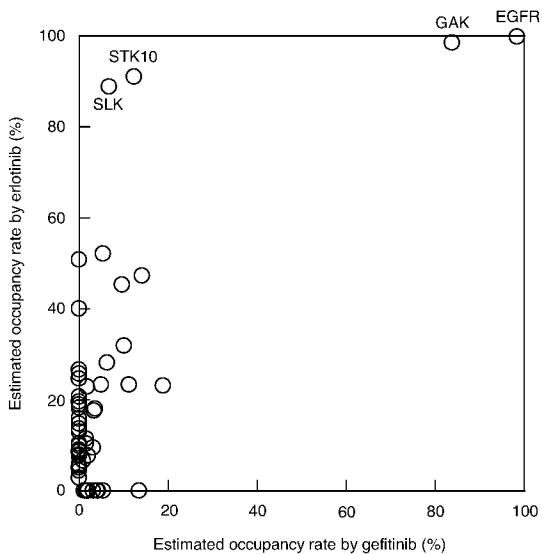


Fig.2

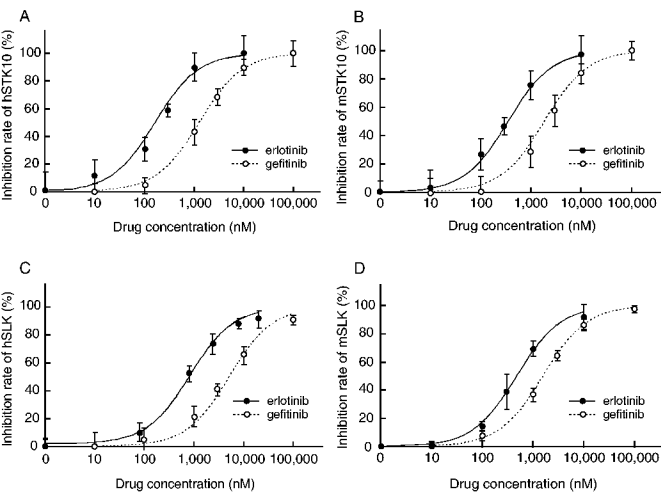
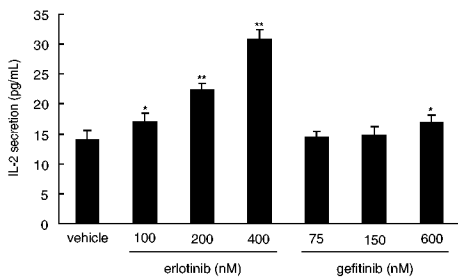


Fig.3

A



B

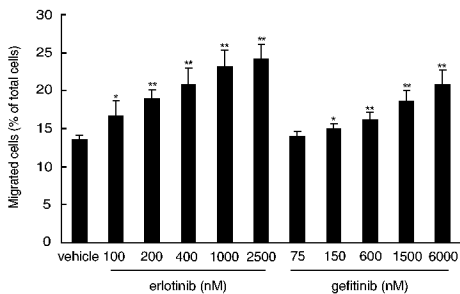


Fig.4

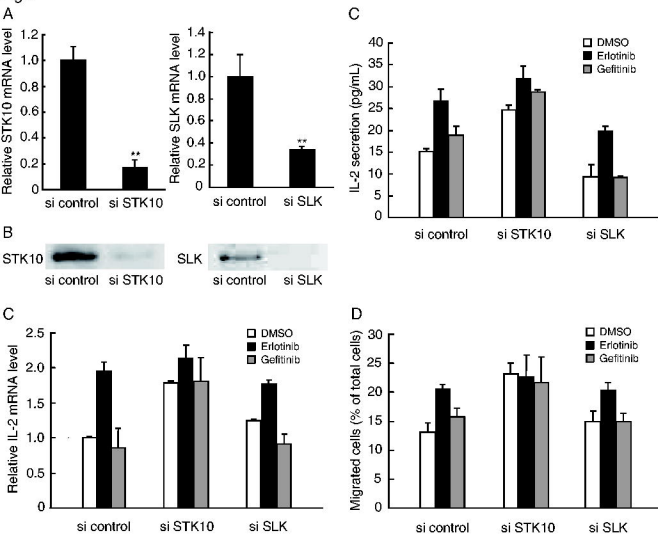


Fig.5

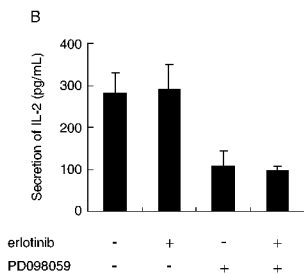
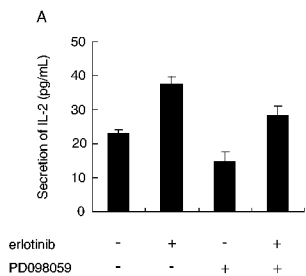


Fig.6

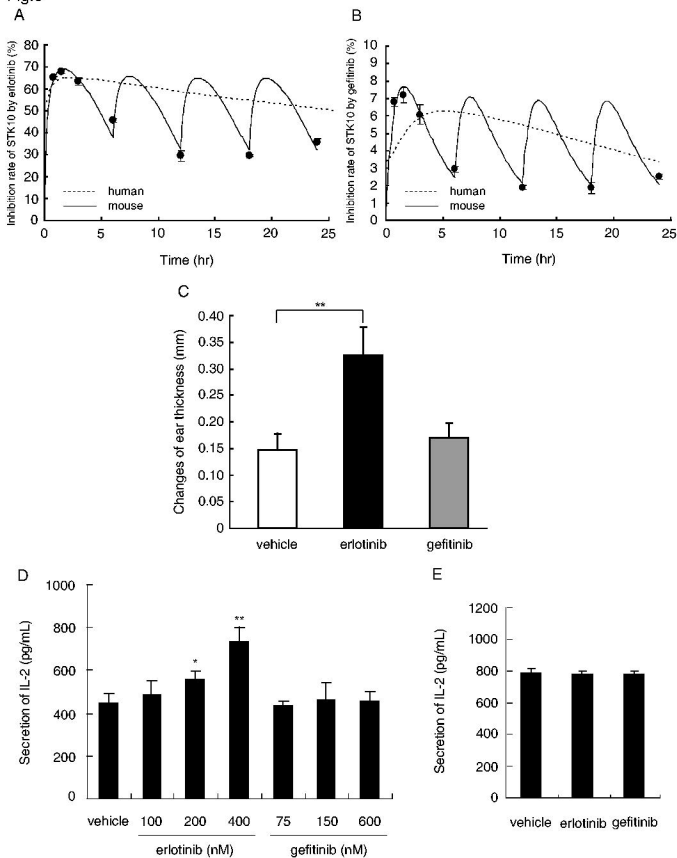


Fig.7 A

